Desalination and Water Treatment
www.deswater.com
doi: 10.1080/19443994.2014.940654

55 (2015) 3188–3194
September

Taylor & Francis
Taylor & Francis Group

Dynamic model of an helical double-pipe evaporator using second-order approach in temporal terms

Mariano Colorado-Pineda[a], F. Alejandro Alaffita[a], Dario Colorado[b,*], Beatris A. Escobedo-Trujillo[a]

[a]*Facultad de Ingeniería, Universidad Veracruzana, Av. Universidad km 7.5, Col. Santa Isabel, Coatzacoalcos, Veracruz C.P. 96535, Mexico*
[b]*Centro de Investigación en Recursos Energéticos y Sustentables, Universidad Veracruzana, Av. Universidad km 7.5, Col. Santa Isabel, Coatzacoalcos, Veracruz C.P. 96535, Mexico, Tel. +921 203 65 16; email: dcolorado@uv.mx (D. Colorado)*

Received 5 March 2014; Accepted 16 June 2014

ABSTRACT

A dynamic model to describe the thermo-hydraulic fluid behavior of a helical double-pipe vertical evaporator with a second-order approach in temporal terms was presented. The model considers equations of continuity, momentum, and energy in each flow; these based on control volume formulation. Liquid phase, two-phase, and vapor flow were considered in the analysis. Conduction in the internal pipe is assumed with a second-order approach in the temporal terms. Also, the heat transfer in the external wall is considered adiabatic. Governing balance equations are discretized. Thermo-physical properties of water were calculated in each point of mesh. Numerical results with the first- and second-order approximation in temporal terms are compared considering the computer's consumption time. Typical perturbations of thermal and fluid flow in the two-phase flow were presented for a double-pipe vertical evaporator. The evaporator is part of a water purification system coupled to a heat transformer. The aim of this work is to identify the advantages of second-order temporal approach.

Keywords: Heat transformer; Simulation time; Water purification

1. Introduction

At the present time, the investigation into new forms of energy conversion is a priority. The absorption heat transformer is a device capable of producing useful heat at a thermal level superior to the one at the source. For this rises the temperature of the source to a more useful level, it is necessary to implement the system with a small amount of energy, such as mechanical energy or thermal energy at high temperature, according to the type of heat transformer [1].

The main components of the heat transformers are: an evaporator, an absorber, a generator, and a condenser. Experimental rig of heat transformer has been studied by different authors. Huicochea and Siqueiros [1] were reported the experimental test results for the first water purification system of single-effect

*Corresponding author.

Presented at the Conference on Desalination for the Environment: Clean Water and Energy 11–15 May 2014, Limassol, Cyprus

evaporation integrated to a heat transformer of 700 W. Sekar and Saravanan [2] were described an absorption heat transformer working with a water–lithium bromide solution coupled with a seawater distillation system. A maximum coefficient of performance of 0.38 and a maximum temperature lift of 20˚C have been reached under operation conditions, the quality of the water is acceptable such as the drinking water according to the Bureau of Indian Standard.

The COP is defined as the ratio of heat delivered in the absorber divided by the heat load supplied to the generator plus evaporator (see Eq. (1)).

$$\mathrm{COP} = \frac{Q_{\mathrm{AB}}}{Q_{\mathrm{GE}} + Q_{\mathrm{EV}}} \tag{1}$$

The study of the thermo-hydraulic behavior in the evaporator is important, because the coefficient of performance is a function of the dynamic state of this system. In this work, special attention has been given to the evaporator under typical thermal and fluid flow disturbances, characteristics of operating range of the heat transformer. For a heat transformer, the operation conditions of absorption are a function of vapor conditions received from the evaporator. Consequently, the pure water steam could be maintained by steady-state heat flow in the absorber.

Two-phase flow is presented in the internal pipe of the evaporator. The two-phase flow has been studied by different authors. Pantankar [3] presented a numerical solution of heat transfer and fluid flow considering continuity, momentum, and energy balance equations coupled. Two-phase flow simulation has been thoroughly studied by several authors using finite volume formulation. Sripattrapan and Wongwises [4] have been presented a mathematical model considering adiabatic steady-state and one-dimensional flow of refrigerants evaporating under constant heat flux in horizontal tubes. García-Valladares et al. [5] reported numerical criteria which allow the simulation, in both steady and transient state, of the thermal and fluid dynamic behavior of double-pipe evaporators and condensers are considering pure refrigerants and mixtures. Colorado et al. [6] presented a physical model to describe heat transfer and fluid dynamic behavior inside a helical double-pipe vertical evaporator, used in the flame of heat pump technology. Gamodel Valladares et al. [5] and Colorado et al. [6] have considered a first-order approach of temporal terms. Escobar et al. [7] presented the thermodynamic theoretical model. It allows the estimation of the coefficient of performance online considering disturbances in the evaporator; the authors suggest develop improvements in the model with the aim of future control.

In agreement to the author's knowledge, there are models of evaporators based on finite volume formulation assuming one-dimensional flow and the first-order approach of temporal terms. Consequently, this work presents, for the first time, a model of two-phase flow based on an approximation of second order in temporal terms. The model is compared with numerical results obtained with the first-order approximations in temporal terms; special attention was made to computer's consumption time. All previous, with the aim of have faster dynamic prediction of heat transfer and pressure drop in helical double-pipe vertical evaporator.

In this paper, is presented the experimental design of helical double-pipe evaporator, mathematical model assuming the second-order approach in temporal terms, numerical solution implemented, the main results comparing first versus. second-order approach in temporal terms and finally, the conclusions.

2. Experimental equipment

Experimental database provided by Santoyo-Castelazo and Siqueiros [8] consist of the information of the heat transformer. Colorado et al. [6] used experimental database for helical double-pipe vertical evaporator. This work used the same experimental conditions.

Helical double-pipe evaporator was built for the heat transformer with stainless steel tubes. The heat exchanger was well isolated by foam insulation. Table 1 describes the geometry of the helical evaporator. In the internal pipe, working fluid flow (water), the evaporation process was carried out, taking into account the heat from the heating water (annulus).

Fig. 1 show the input and output stream in the evaporator. The working fluid, water, in the evaporator inlet (E2), which comes from condenser changes of phase, and it is transformed in outlet vapor (S2) goes to absorber.

The experimental information is as follows: the instrumentation of mass flow rate was not implemented for internal pipe; only mass flow rate is registered for the annulus pipe. A manovacuometer Bourdon-type was employed to measure the pressure

Table 1
Double-pipe vertical evaporator main data

	Internal pipe (mm)	External pipe (mm)
External diameter	19.2	32.7
Internal diameter	16.9	29.1
Helical diameter	400	400
Turns	4.5	4.5
Length	5,655	5,655
Height	310	310

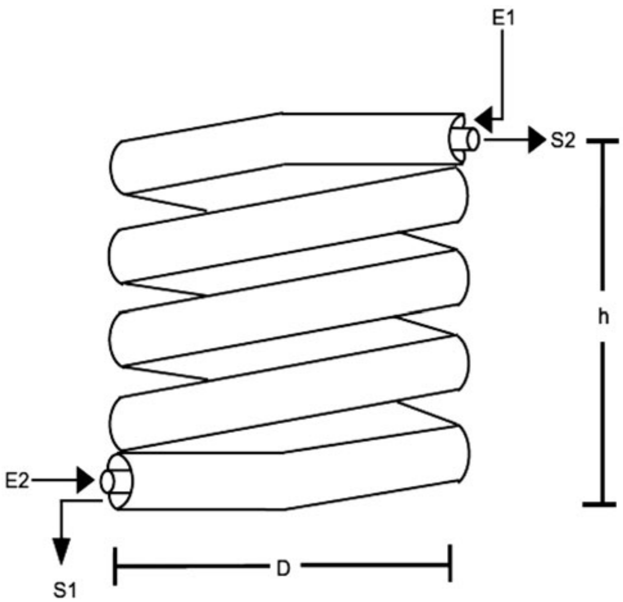

Fig. 1. Sketch of the experimental test section.

in the inlet vapor from the absorber. The general assumption is that the outlet pressure from the evaporator is equal to the registered at the inlet vapor from the absorber. In order to register the bulk temperature, four thermocouples T-type (copper-constantan) were installed at the inlet and outlet flows (in positions E1, S1, E2, and S2) of the evaporator. The experimental measurement is shown in Table 2.

3. Mathematical models

In this section, mathematical formulation of two-phase flow assuming second-order approach in temporal terms is presented. Taking into account the characteristic helical coils, governing equations were integrated following these assumptions. We suppose that under or assumptions the governing equations for two-phase flow are given as: one-dimensional flow, non-participant radiation medium and negligible radiant heat exchanger between surfaces, axial heat conduction inside the fluid is neglected, internal and coiled diameter constant, and uniform roughness surface. Our setting present:

3.1. Continuity equation

States that the change in rate of mass, $\frac{\partial m}{\partial t}$ within control volume plus the net mass flow, M, through a control surface is zero [9], i.e.

$$0 = M + \frac{\partial m}{\partial t} \tag{2}$$

3.2. Momentum equation

It is the sum of the forces of the volume with respect to the change in the time of the control volume and the accumulation moment [10].

$$\Delta PA - \tau P \Delta z + y \partial z \partial y \sin\theta = vM + v\frac{\partial m}{\partial t} \tag{3}$$

where ΔPA is the differential pressure that crosses an area A; $\tau P \Delta z$ where the tensions are passing through the area; $y\partial z \partial y \sin\theta$ is the volume flow; vM is velocity of the mass flow through the surface control and $v\frac{\partial m}{\partial t}$ is velocity of the mass flow with change in rate overtime.

3.3. Energy equation

It is for a system or a cycle is the total heat that the system acquires from the surrounding region and it is proportional to the work done by the system [10].

$$Q - W = eM + e\frac{\partial m}{\partial t} \tag{4}$$

where Q is the heat system, W is the work done by the system, eM is energy that passes through the mass flow control surface, and $e\frac{\partial m}{\partial t}$ is energy that goes into the control volume.

Table 2
Instrumental uncertainties of physical quantities

Instruments	Error	Measurements scale
Rotameter	±3%	Punctual scale
Bourdon Manovacumeter	±0.5%	Full scale (0.033–2.07 bar)
Thermocouples T-type	±0.5	Punctual scale

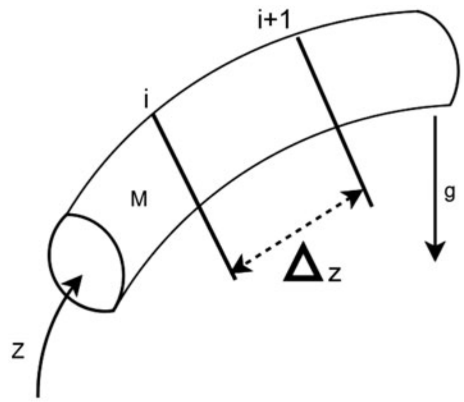

Fig. 2. Control volume.

differential scheme as: $\frac{3\phi_{k-2}-4\phi_{k-1}+\phi_k}{2\Delta t}$, where: represents a generic ($\phi = m, h, p$) dependent variable in the present moment calculation, ϕ_{k-1} indicates its value in the previous time and ϕ_{k-2} is the value at two previous moments. The discretized mass, momentum, and energy equations are:

$$M_{i+1} = M_i - \frac{\Delta z A}{2\Delta t}(3\rho_{k-2} - 4\rho_{k-1} + \rho_k) \tag{5}$$

$$P_{i+1} = \frac{P_i}{A} - P\tau\Delta z - \frac{\rho}{A} - \frac{\Delta z v}{2\Delta t}(3\rho_{k-2} - 4\rho_{k-1} + \rho_k) \tag{6}$$

$$\begin{aligned} q(P_{i+1} - P_i)\Delta z = {} & (M_{gi+1})(h_{i+1} - h_i) + M(h_{i+1} - h_{li}) + (m_{gi+1} - m_{gi} + m_{li+1} - m_{li}) \\ & - \frac{[3(h_{i+1} - h_i)_{k-2} - 4(h_{i+1} - h_i)_{k-1} + (h_{i+1} - h_i)_k]}{2\Delta t} - \frac{A\Delta z[3(P_{i+1} - P_i)_{k-2} - 4(P_{i+1} - P_i)_{k-1} + (P_{i+1} - P_i)_k]}{2\Delta t} + h_{i+1} \\ & - h_i \frac{[3(m_{i+1} - m_i)_{k-2} - 4(m_{i+1} - m_i)_{k-1} + (m_{i+1} - m_i)_k]}{2\Delta t} \end{aligned} \tag{7}$$

Fig. 2 shows a control volume, where subscripts "i" and "$i+1$" represent the cross-sections of input and output, respectively. The governing equations for two-phase flow: integrated Eqs. (2)–(4), are considered in two domains in the liquid phase and a vapor phase, so we obtain new equations.

$$0 = M_{i+1} - M_i + \frac{\partial m}{\partial t}$$

$$P_{i+1} = \frac{P_i}{A} - P\tau\Delta z - \frac{\rho}{A} - v\frac{\partial m}{\partial t}$$

$$qP\Delta z = \boldsymbol{\vartheta}_g h + Mh_l + \gamma\frac{\partial \chi}{\partial t} - A\Delta z\frac{\partial P}{\partial t} + h_l\frac{\partial \gamma}{\partial t}$$

where
$\boldsymbol{\vartheta}_g = M_{g_{i+1}}$; $\chi = m_g + m_l$; $\gamma = h_g + h_l$ and $\frac{\partial m}{\partial t} = \frac{\Delta z A \rho}{\Delta t}$ (see [8] for details) too.

The domain of flow is divided into control volumes. Therefore, we have implemented one implicit scheme for transient equations terms and the governing equations are discretized assuming a Empirical information is required for the governing equations solutions, in this work, the void fraction, friction factor, and convective heat transfer coefficient are assumed in accordance with Colorado et al. [6]. This was based on the formulation of the first order that García-Valladares [11] equations described.

4. Numerical solution

The discretized governing equations were coupled using a fully implicit "step by step" method in the flow direction. For each variable, control volume outlet value is iteratively obtained from the corresponding inlet value. The output of every node is used as input for the downstream node. This procedure is followed until the end of the helically coiled tube is reached. The temperature distribution in the internal wall is calculated assuming a second-order approach in temporal terms with the temperature distribution in the flow and heat transfer coefficients using a tri-diagonal matrix algorithm. Inside each control volume, strict convergence of numerical calculations was verified. The required boundary conditions are mass flow, enthalpy, and pressure in the internal and annulus inlets. Heat exchange does not occur between the system and the environment. Steady-state solution is a particular case and starting point of dynamic model. In this work, the disturbances have been incorporated into the model as step changes.

5. Results and discussion

The proposed model represents the two-phase flow, Eqs. (5)–(7). The algorithm is well developed as it gives the same results that the experimental data mentioned by Santoyo and Siqueiros [7]. The initial conditions were 37.9˚C and 46 kPa for inlet of internal tube.

Fig. 3 shows pressure simulated against the length of internal pipe. Experimental pressure at the inlet of the absorber in the heat transformer was plotted.

With the aim to evaluate the two-phase flow mathematical formulation above, this work considered typical disturbance in the inlet of internal tube. The disturbance could be caused by two reasons: first, the heat load and fluid flow changes in the condenser and second, for the variations of operation conditions in the absorber–generator cycle. In this way, we considered four disturbances as following: (a) the same temperature will start to rise as an experimental condition described previously, but will have increased pressure to 47 kPa, (b) the inlet temperature was 47˚C and an increase in the pressure to 47 kPa, (c) the temperature as the experimental conditions (37.9˚C) and a decrease in pressure to 45 kPa is reached, finally, (d) temperature increased to 47˚C and the pressure decrease to 45 kPa. Disturbances in the input conditions of the working fluid are assumed according to typical operation conditions of the heat transformer.

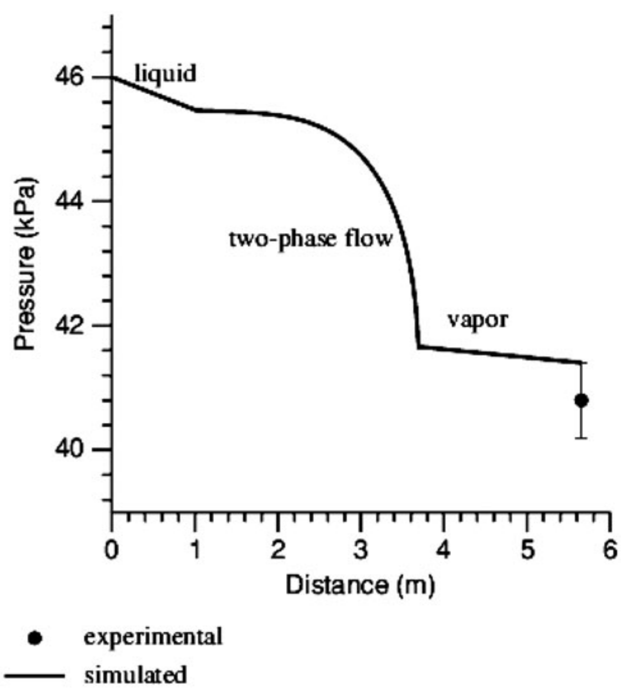

Fig. 3. Experimental versus simulated data by Santoyo-Castelazo and Siqueiros [8] in steady state.

Table 3
Comparisons of the time step with different mesh sizes $\left(I = 100 - \frac{\varphi^2(100)}{\varphi^1}\right)$

Perturbations	Nodes	I (%)
(a)	200	12.33
(b)	200	14.55
(c)	200	17.17
(d)	200	8.05
(a)	150	13.56
(b)	150	16.35
(c)	150	14.37
(d)	150	12.76
(a)	100	13.21
(b)	100	15.74
(c)	100	13.76
(d)	100	14.75
(a)	50	14.32
(b)	50	15.78
(c)	50	16.84
(d)	50	16.79

Several simulations with different mesh sizes were carried out. Table 3 shows the results of improvement coefficient I. The improvement coefficient compared the computer's consumption time for model assuming first- and second-order approach.

For (a–c) the disturbances of improvement coefficient is practically constant of 13, 15.6, and 15.53%, respectively, it is independent from the number of control volumes. For (*d*) disturbance, the improvement percent increase up to 108.6% changing the number of control volumes from 200 to 50. The dynamic states from 0 to 200 s were assumed.

A dynamic model was used to describe thermo-hydraulic behavior with inlet disturbance of internal pipe. In Fig. 4, the outlet pressure was seen at each time. This figure is divided into four sections each having the perturbations that were discussed above. These simulations were carried out with a mesh of 200 nodes, a time step of 5 s, and convergence criteria of 1×10^{-3}. The model assuming the first- and second-order approach of temporal terms presented the same final numerical results.

In Fig. 4, it can be seen that the outlet pressure is practically independent of the inlet temperature perturbation. Significant changes in outlet pressure occur from 0 to 90 s, then after this time the system is

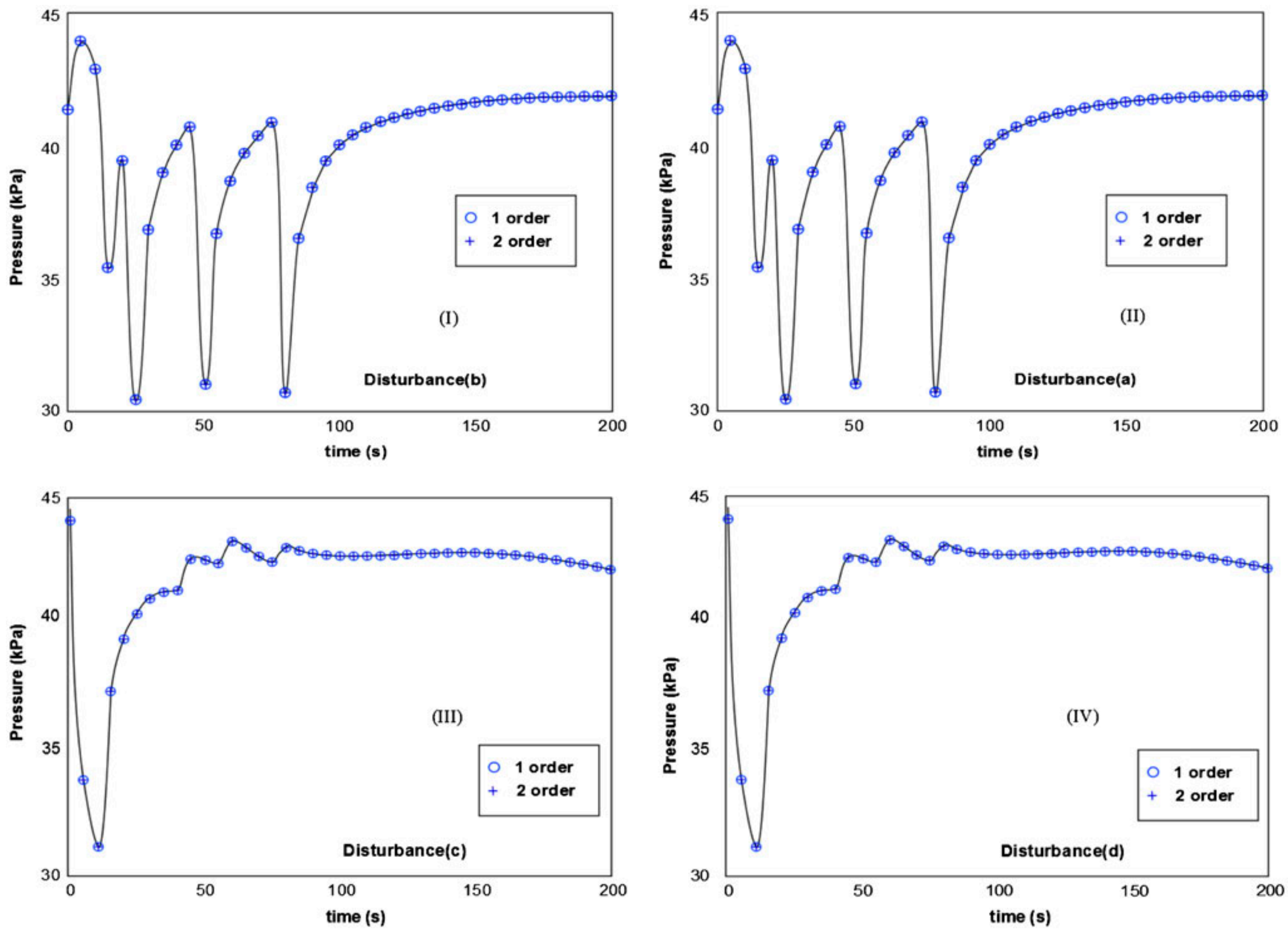

Fig. 4. System pressure disturbances in the outlet of evaporator.

assumed as stable. Oscillations that occur in Fig. 4 are caused by the change of two-phase flow volume in the internal pipe. The change of two-phase flow affects the output pressure each time. Thus, we can see that if the pressure increases a greater oscillation is presented, as the case shown in Fig. 4. However, if the pressure decreases the oscillation is less, as the case shown in Fig. 4. In according with the numerical results, small amplitude oscillations are reached, when the evaporator decreased the pressure. So, to achieve a constant heat transfer in the absorber and consequently reach continuous production of water purification is recommended to decrease the inlet pressure in the evaporator.

6. Conclusion

The effect of temperature and pressure perturbation based on first- and second-order approach in the temporal terms of the two-phase flow for a helical evaporator was carried out. The inlet pressure perturbation exhibited significant oscillations of outlet vapor pressure from 0 to 90 s.

It was observed that the mathematical model with a second-order approach in the temporal term has a gain of computing time up to 17.2%. Further studies will try to adapt this dynamic model assuming second-order approach in temporal terms for heat transformer technologies, with the objective of future control and online estimation of COP decreasing the simulation time as well as the inclusion of disturbance in the heat transformer and its effect on the water purification process. According to the mathematical formulation of two-phase flow presented in this work, it is possible to make use of other fluids, mixtures, and operating conditions; it allows using the model developed as a tool to design and optimize these kinds of systems.

Acknowledgment

This study has been supported by PROMEP (proyect number: P/PROMEP/103.5/13/7,135). The authors thank the Engineering Faculty of Universidad Veracruzana, campus Coatzacoalcos, for partial economical support.

Nomenclature

A	—	cross-section area [m^2]
AB	—	absorber
b	—	coil pitch
CO	—	condenser
COP	—	coefficient of performance [dimensionless]
CV	—	control volume
D	—	helical diameter [m]
d	—	internal diameter [m]
e	—	specific energy $\left[h+\frac{V^2}{2}+g\sin\theta\right]\left[\frac{J}{kg}\right]$
EV	—	evaporator
f	—	friction factor
g	—	acceleration due to gravity $\left[\frac{m}{s^2}\right]$
GE	—	generator
h	—	enthalpy $\left[\frac{J}{kg}\right]$
M	—	mass flow rate $\left[\frac{kg}{s}\right]$
m	—	mass [kg]
n_z	—	number of control volumes
P	—	pressure [Kpa]
p	—	perimeter [m]
q	—	heat flux per unit of area $\left[\frac{W}{m^2}\right]$
Q	—	heat flux [kW]
t	—	time [s]
T	—	temperature [°C]
	—	velocity $\left[\frac{m}{s}\right]$
x_g	—	vapor mass fraction
z	—	axial coordinated
Greek letters		
α	—	heat transfer coefficient [$\frac{W}{m^2}$°C]
Δt	—	temporal discretization step [s]
Δz	—	axial discretization step [m]
∂	—	convergence criterion [dimensionless]
ε_g	—	void fraction
θ	—	angle [rad]
ϑ	—	output steam mass flow
μ	—	dynamic viscosity [Pa s]
τ	—	two-phase frictional multiplier
ρ	—	density $\left[\frac{kg}{m^3}\right]$
φ^2	—	second-order temporally
φ^1	—	first-order temporally
ϕ	—	variable generic
X	—	mass flow in two phase
Subscript		
g	—	vapor
l	—	liquid
$i+1$	—	output control volume
i	—	input control volume

References

[1] A. Huicochea, J. Siqueiros, Increase of COP for an experimental heat transformer using a water purification system, Desalin. water Treat. 12 (2009) 305–312.

[2] S. Sekar, R. Saravanan, Experimental studies on absorption heat transformer coupled distillation system, Desalination 274 (2011) 292–301.

[3] S.V. Pantankar, Numerical Heat Transfer and Fluid Flow, CRC-press, Boca Raton, FL, 1980.

[4] W. Sripattrapan, S. Wongwises, Two-phase flow of refrigerants during evaporation under constant heat flux in a horizontal tube, Int. Commun. Heat Mass 32 (2005) 386–402.

[5] O. García-Valladares, C.D. Perez Segarra, J. Rigola, Numerical simulation of double pipe condenser and evapoarator, Int. J. Refrig. 27 (2009) 656–670.

[6] D. Colorado-Garrido, E. Santoyo-Castelazo, J.A. Hernández, O. García-Valladares, J. Siqueiros, D. Juarez-Romero, Heat transfer of a helical double-pipe vertical evaporator; Theoretical analysis and experimental validation, Appl. Energy 86 (2009) 1144–1153.

[7] R.F. Escobar, J.A. Hernández, C.M. Astorga-Zaragoza, D. Colorado, D. Juárez, Analysis of the evaporator heat flow rate in a water purification process integrated to an absorption heat transformer with energy recycling, Desalin. Water Treat. 5 (2009) 59–67.

[8] E. Santoyo-Castelazo, J. Siqueiros, Estudio experimental de un sistema de purificación de agua integrado a un transformador térmico Memorias del XXVIII Encuentro (Experimental study of a water purification system integrated of a heat transformer, Memories of XXVIII AMIDIQ), Nacional de la, AMIDIQ, TER-21, Manzanillo, 2007, pp. 4072–4085.

[9] Y.A. Cengel, M.A. Boles, Thermodynamics, fourth ed., McGrawHill, New York, NY, 2001.

[10] J.R. Welty, C.E. Wicks, R.E. Wilson, Fundamentos de Transferencia de Momento (Fundamentals of mometum, heat and mass transfer), Calor y Masa, Limusa, 1994.

[11] O. García-Valladares, Numerical simulation and experimental validation of coiled adiabatic capillary tubes 27 (2007) 1062–1071.